Bone Reports 18 (2023) 101680

Contents lists available at ScienceDirect

Bone Reports

journal homepage: www.elsevier.com/locate/bonr

Type 2 diabetes alters the viscoelastic behavior and macromolecular composition of vertebra

Deepak Mehta [a], Praveer Sihota [a], Kulbhushan Tikoo [b], Sachin Kumar [a,*], Navin Kumar [a,*]

[a] Department of Mechanical Engineering Indian Institute of Technology Ropar, India
[b] Department of Pharmacology and Toxicology, National Institute of Pharmaceutical Education and Research Mohali, India

ARTICLE INFO

Keywords:
Vertebral body
Creep
Stress relaxation
Molecular structure
ATR-FTIR
XRD

ABSTRACT

Type 2 diabetes (T2D) affects the functional behavior of vertebra bone by altering its structural and mechanical properties. The vertebral bones are responsible to carry the body weight and it remains under prolonged constant load which results to viscoelastic deformation. The effect of T2D on the viscoelastic behavior of vertebral bone is not well explored yet. In this study, the effects of T2D on the creep and stress relaxation behavior of vertebral bone are investigated. Also, this study established a correlation between T2D associated alteration in macromolecular structure and viscoelastic behavior of vertebra. In this study T2D female rat SD model was used. The obtained results demonstrated a significant reduction in the amount of creep strain ($p \leq 0.05$) and stress relaxation ($p \leq 0.01$) in T2D specimens than the control. Also, the creep rate was found significantly lower in T2D specimens. On the other hand, molecular structural parameters such as mineral-to-matrix ratio (control vs T2D: 2.93 ± 0.78 vs 3.72 ± 0.53; $p = 0.02$), and non-enzymatic cross link ratio (NE-xL) (control vs T2D: 1.53 ± 0.07 vs 3.84 ± 0.20; $p = 0.01$) were found significantly altered in T2D specimens. Pearson linear correlation tests show a significant correlation; between creep rate and NE-xL ($r = -0.94$, $p < 0.01$), and between stress relaxation and NE-xL ($r = -0.946$, $p < 0.01$). Overall this study explored the understanding about the disease associated alteration in viscoelastic response of vertebra and its correlation with macromolecular composition which can help to understand the disease related impaired functioning of the vertebrae body.

1. Introduction

Type 2 diabetes (T2D) is the most common disease with several comorbidities which increases the world global health burden (Sihota et al., 2020). T2D can be identified by high blood glucose level resulting from insulin resistance and/or relative insulin deficiency (Care and Suppl, 2019). The chronic hyperglycemic state in T2D causes the production of advanced glycation end-products (AGEs) in the tissue. The accumulation of AGEs may affect the musculoskeletal composition by modifying the extracellular matrix and impairing cellular homeostasis (Tsai et al., 2014). T2D has altered native function of all tissues which causes the damage of tissues from head-to-toe: heart, kidney, nerves, eye, skin, tendon, blood vessels, intervertebral disc, cartilage, spine, and bone (Sihota et al., 2020; Brownlee, 1995; Lakhani et al., 2023; Wyatt and Ferrance, 2006; Molsted et al., 2012; Liu et al., 2018; Kurra and Siris, 2011; Anekstein et al., 2010; Yamamoto et al., 2009; Yadav et al., 2021; Sihota et al., 2021). Our previous study has developed a high-fat diet (HFD)-fed and low-dose streptozotocin (STZ)-treated T2D rat model (Sihota et al., 2020). In this study, genetically normal outbred female Sprague Dwaley (SD) rats were used to investigate the effect of T2D on the microstructure and mechanical properties of the femoral bone. This study demonstrated that diabetes affects each hierarchy level of the bone and deteriorates its mechanical behavior. Some Other studies demonstrated the alteration in microstructure (e.g., mineral density, mean crystal size, cortical porosity, trabecular microstructure, protein structure/content (amide-I, and amide-II)) and mechanical properties (e.g., yield stress, apparent modulus, maximum stress, toughness to maximum stress, post yield toughness, fracture toughness) of bone (Sihota et al., 2020; Brownlee, 1995; Lakhani et al., 2023; Wyatt and Ferrance, 2006; Molsted et al., 2012; Liu et al., 2018; Kurra and Siris, 2011; Anekstein et al., 2010; Yamamoto et al., 2009; Yadav et al., 2021; Sihota et al., 2021; Karim et al., 2018; Hunt et al., 2019; Wölfel et al., 2020; Piccoli et al., 2020; Gallant et al., 2013; Rubin et al., 2016; Acevedo et al., 2018; Hunt et al., 2018). Out of the above mentioned tissue (e.g, heart, kidney, nerves, eye, skin, tendon, blood vessels, intervertebral disc, cartilage, spine, and bone), the vertebral bodies with its

* Corresponding authors.
E-mail addresses: sachin@iitrpr.ac.in (S. Kumar), nkumar@iitrpr.ac.in (N. Kumar).

https://doi.org/10.1016/j.bonr.2023.101680
Received 7 January 2023; Received in revised form 1 April 2023; Accepted 19 April 2023
Available online 25 April 2023

complex structure are thought to be more susceptible to the detrimental effects of T2D. The patients with T2D report more spinal pathologies including spinal stenosis (Anekstein et al., 2010), osteoporosis (Kurra and Siris, 2011), poor post-operative outcomes of lumbar fusion (Browne et al., 2007), and vertebral fracture (Kurra and Siris, 2011; Yamamoto et al., 2009).

Vertebra is primary load carrying and transmitting structures in the axial skeleton and it is composed of cortical and cancellous bone. The alteration in mechanical properties of vertebra may lead to loss in its native functions as the damage or fracture of vertebra are directly associated with the loss of its native mechanical and structural properties (Miyake et al., 2018; Klotzbuecher et al., 2000), as these studies reported reduced bone mineral density (BMD) and then increase fracture risk in T2D patients. The vertebral fractures are associated with higher mortality (Miyake et al., 2018; Kanazawa et al., 2009). Other studies investigated the irreversible residual strain, creep and damage of vertebra body under long term static and cyclic loading and reported time associated residual strain and damage which may be cause of age associated non traumatic fracture of vertebra body (Yamamoto et al., 2006; Kim et al., 2011; Gustafson et al., 2017; O'Callaghan et al., 2018; Pollintine et al., 2009; Keaveny et al., 1994; Robinson et al., 2021). Other works also reported compromised mechanical properties of vertebra such altered stiffness, ultimate compressive strength and toughness as result of T2D (Gallant et al., 2013; Yamamoto et al., 2006; Robinson et al., 2021; Reinwald et al., 2009; Li et al., 2017). Many others investigated the effect of T2D on the micro and molecular structure of vertebrae/bone (Yadav et al., 2021; Sihota et al., 2021; Rubin et al., 2016; Xue et al., 2018) and found significant deterioration in structure quality such as reduction in BMD, bone volume fraction, collagen quality etc.

Beside the significant amount of work on effect of T2D on mechanical and structural properties of vertebra, the question, does T2D affect the viscoelastic behavior of vertebrae, remains poorly answered. Also, the correlation between change in molecular structure of vertebrae due T2D and its viscoelastic properties was not explored well. However, knowledge about these aspects is utmost important for proper clinical care. Though, it is well documented that the vertebrae bone is viscoelastic material (Kim et al., 2011; Oravec et al., 2018) and this mechanical property plays a crucial role to sustain the prolonged load in static (walking) and dynamic (running) physiological conditions. Also, the available clinical studies indicate that progressive vertebral deformation of elderly patients results in long-term vertebral height loss which results in back pain (Briggs et al., 2004; Melton and Kallmes, 2006). The long term creep eventually leads to vertebrae fracture (Keller et al., 2003; Sone et al., 1997). Further, Kim et al. (2011) investigated the relationship between microstructure and creep behavior of the vertebrae. This study shows a strong correlation between tissue mineral density and creep rate of the tissue. Also, it is well documented that the T2D affects the microstructure of the tissue. The available research gap motivate use to understand the effect of T2D on the viscoelastic behavior of vertebra and correlation between viscoelastic properties and macromolecular structure vertebra.

The aim of current study is to investigate the effect of T2D on the viscoelastic property and molecular structure of rat vertebra. We also investigated the relationship between alteration in molecular structure and viscoelastic property of the tissue. Here, we used a HFD-fed and low-dose STZ-treated T2D rat model to test vertebrae of the healthy and diabetic rat under compression loading to capture the time dependent behavior of the tissue. In this regard the creep and stress relaxation tests were performed on the control and T2D vertebrae bone by using a uniaxial compression test. The alteration was observed in collagen molecule, mineral to matrix ratio, cross linking (non-enzymatic cross linking) and crystal size (crystals were quantified using FTIR-ATR, and XRD). A correlation between the mechanical and structural properties of vertebra was established by using statistical tool.

2. Material and methods

2.1. Animals

The study was started with six-eight week old female Sprague Dawley rats (190–200 g), which were collected from the central animal facility of NIPER (National Institute of Pharmaceutical Education and Research, Mohali, India). All animals were accustomed to a new environment (~20° temperature, and ~50 % relative humidity) for one week and 12 h of light and dark cycle with food and water ad libitum. All protocol design for the experiments of this study were approved by the Institutional Animal Ethics Committee (IAEC approval Number 17/75, NIPER) and these protocols were performed in accordance with the guidelines of the Committee for the Purpose of Control and Supervision of Experiments on Animals (CPCSEA), New Delhi, India. The brief scheme to induce diabetes is provided in Fig. 1(A) and comparison of blood glucose parameters to confirm the T2D in rats is provided in Fig. 1 (B).

2.2. Experimental design and sample preparation

The detail about the experimental procedure to induce T2D in the animal was explained in our previous published study (Sihota et al., 2020). The spines (L1-S1) of control and T2D animal were excised using the scalpel. After cleaning the adjacent soft tissues, the L4 vertebrae of all animals were separated by slicing through the adjacent intervertebral disc. Total twenty four specimens (twelve in control and twelve in T2D) were taken for creep experiments and sixteen specimen (eight control rat and eight T2D rat). All specimens were wrapped in PBS shocked gauge and stored properly at −20 °C till the experiment.

Specimens of equal length with parallel surfaces are required for accurate mechanical compression tests. The parallel surfaces ensure full contact with the loading grips and allow uniform distribution of applied load over the specimen surfaces and eliminates the unwanted error in mechanical response. However, obtaining of true parallel surfaces and equal gauge length for all specimens is not easy for such small samples. Hence, we designed a special method to cut the specimens of equal size with parallel surfaces. Here, two symmetric steel plates (5.5 mm thickness) with semicircular holes of different diameters were fabricated, the

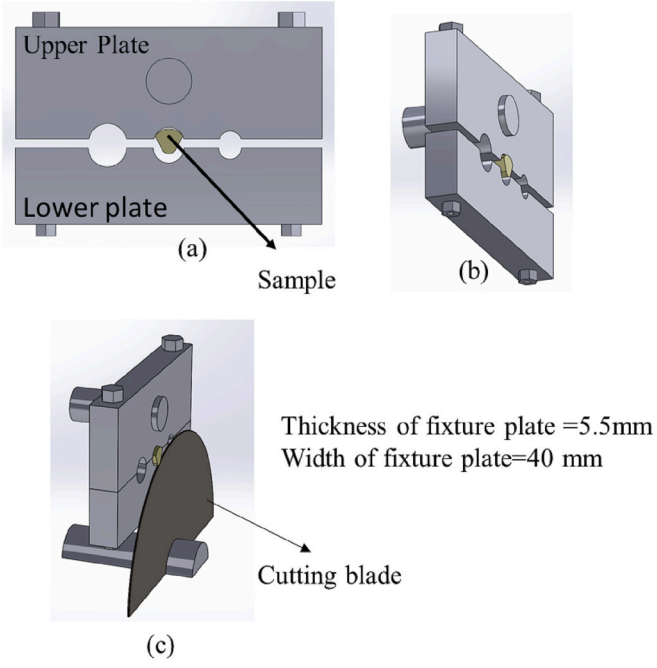

Fig. 1. Representation of specimen cutting procedure.

vertebra of different size (cross-section) were tightened (Fig. 1) (Note. tightening force was applied very gently to avoid any damage and lateral deformation) between these two plates inside the hole of corresponding dimensions. The complete assembly was then mounted on the low-speed diamond blade saw (IsoMet, Buehler, Lake Bluff, IL, USA) and ends of vertebra outside the hole were cut using a diamond saw. After removing the overhanging ends, the length of each specimen was measured and mean length of specimens was found 5.21 ± 0.03 mm. The cross section dimensions were measured using the method as described elsewhere (Li et al., 2017). The cross section was measured at five different locations over the gauge length and the minimum value of cross section area was considered for the stress and strain calculation. The average value of minimum cross section area of control and T2D specimens were 8.53 ± 1.21 mm^2 and 8.37 ± 1.18 mm^2, respectively.

2.3. Experimental procedure

After sequentially thawing the specimen at 4 °C and room temperature, the creep and recovery tests were performed in all specimens of each group. Total four groups (n = 6 in each group) (group-1, and group-2 contained control specimens and group-3, and group-4 carried T2D specimens) were made according to protocol of the experiment. These groups were divided according to creep test protocol as described in next paragraphs (steps for creep and recovery experiments). The experiments were performed using an electromagnetic testing system (Electroforce 3200, Bose, Eden Prairie, MN, USA) (Fig. 2(A)). Prior to the actual test, a preload of 5 N was applied on each specimen to ensure proper contact between grips and specimen surface.

The creep and stress relaxation tests were performed according to the previously described protocols (Pollintine et al., 2009). The creep test consists four different steps: step-1: Specimens of group-1 and group-3 were compressed up to 0.2 % (2000 με) strain while specimens of group-2 and group-4 were compressed up to 0.4 % (4000 με) strain. All specimens were compressed in displacement control with strain rate of 0.01 s^{-1}; Step-2: Once the desired strain was reached, displacement control mode was switched to load control mode and the specimen was held for 400 s at this load value. During this step, the deformation of the specimen was monitored against this hold load; Step-3: specimen was unloaded to zero load with the same strain rate as of loading step; step-4: specimen was held at zero load for 600 s and recovery in deformation was measured (Fig. 2(B)).

For stress relaxation experiments each specimen was compressed up to 0.3 % (3000 με) strain and held for 3600 s. During this hold period, the reduction in load was measured which was later converted into a normalized value of stress. All experiments were performed inside the PBS filled chamber (Fig. 2(A)) and at room temperature to maintain the hydration of tissue during the experiment. The load deformation data were captured at 200 Hz sampling frequency.

2.4. ATR-FTIR

Small biopsy of vertebra (n = 10 samples in each control and T2D) bone was freeze dried for 24 h and using mortar and pestle, freeze dried bone was directly crushed in powder having particle size of few micron. Following this step, the powered particles were scanned under the Bruker IFS 66v/s FTIR spectrometer in Attenuated Total Reflection (ATR) mode. FTIR spectra were recorded in the spectral range of 500 to 4000 cm^{-1} (Fig. 3(A)). All specimens were scanned under constant pressure. Further, the recorded spectra were analyzed by using OriginPro 8 (OriginLab, Northampton, MA) software. After baseline correction, the phosphate band (916–1180 cm^{-1}) and amide-I band (1589–1710 cm^{-1}) were selected to quantify the matrix and collagen related parameters i.e. mineral to matrix ratio, enzymatic cross linking (E-xLR), and non-enzymatic cross linking (NE-xLR). The mineral to matrix ratio was quantified as an area ratio of the phosphate band to amide-1 band, whereas the alteration in "E-xLR", and "NE-xLR" was measured by deconvolution of amide-1 peak which is the location of strongest peaks for non-enzymatic cross-link (NE-xLR) pentosidine (AGE) (Sihota et al., 2020; Sihota et al., 2021).

The amide-1 peak was deconvoluted into six Gaussian sub peaks of 1610, 1630, 1648, 1660, and 1678, and 1690 cm^{-1} by using a peak analyzer tool in Origin-2021 software (Fig. 3(B)). These peaks were found based on the second derivative of obtained spectra of amide-1 peak. From the deconvolution of amide-1 peak, the NE-xLR was quantified by area ratio of 1678/1690 cm^{-1}, whereas E-xLR was quantified using 1660/1678 cm^{-1}. Further, the collagen maturity level was measured using the area ratio of 1660/1690 cm^{-1}. The quantification of NE-XLR is a measurement of collagen quality associated with NE-xLR and is an indirect measure of the overall AGEs contest in the tissue (Schmidt et al., 2017).

2.5. Mean crystallite size (XRD)

The powder of vertebra, used in FTIR analysis was dried in a fume hood and transferred in the tightly sealed cryovials, and XRD spectra of specimens were recorded using the Panalytical X'Pert Pro multipurpose diffractometer (Netherlands). The XRD spectra were recorded at 40 kV and 40 mA in no spinning mode with Cu-tube by CuKa radiation wavelength of 1.506 A^0. All XRD spectra were recorded in the angular range of 2θ = 20° to 45, with a step size of 0.033/2θ and the count time at each step was 250 s. The obtained spectra were background corrected and analyzed using X'pert plus software. After fitting the XRD spectra,

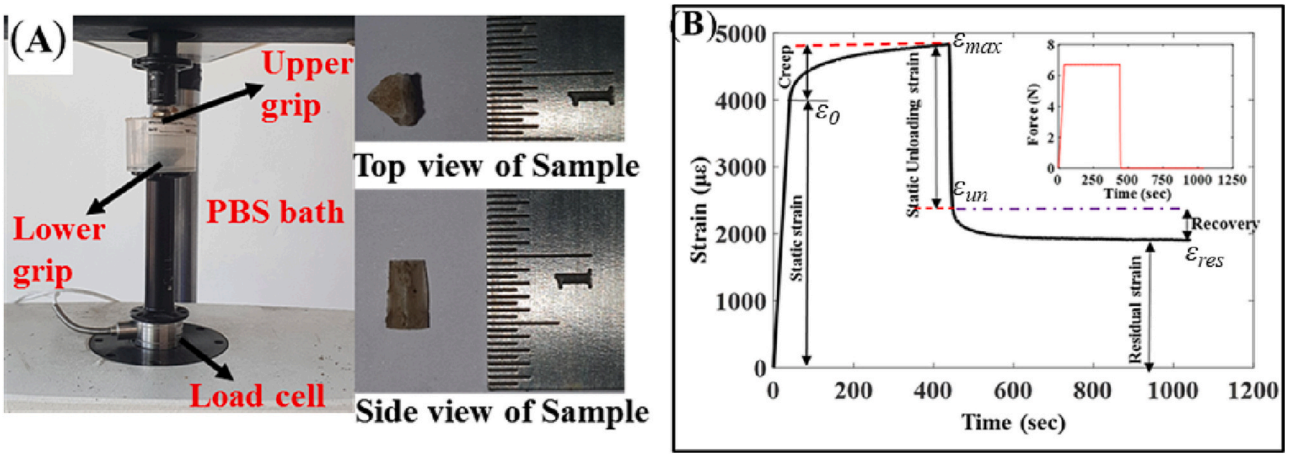

Fig. 2. (A) Demonstrates experimental setup (left side) and dimensions of specimen. (B) Input load steps (in subfigure) and output strain response of the specimen.

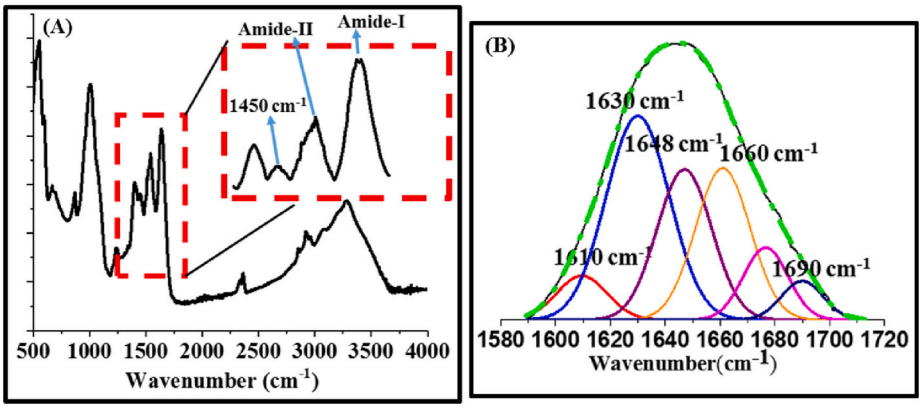

Fig. 3. (A) Representative ATR-FTIR spectrum of vertebra specimen, (B) Representative amide-1 band with six sub peaks. These sub peaks were used to measure the molecular difference between control and T2D vertebra.

peak at $2\theta = 26^{\circ}$ belongs to average length of the crystal, and peak at $2\theta = 40^{\circ}$ belongs to average width of the crystal (Sihota et al., 2020; Sihota et al., 2021). Further, the average crystal size was calculated using the Scherrer Eq. (1).

$$B(2\theta) = \frac{\lambda}{L}cos\theta \tag{1}$$

where B is mean crystal size, λ is x-ray wavelength, θ is the Bragg angle, and L is the peak width at half maximum.

2.6. Experimental data analysis

Displacement and load data obtained from the machine were converted into strain and stress data by dividing the displacement and load data by specimen length and its minimum cross section area, respectively. On the other hand the creep strain was measured using the Eq. (2).

$$\varepsilon_{creep} = \varepsilon_{\max} - \varepsilon_0 \tag{2}$$

where, ε_{creep} is creep strain, $\varepsilon_{\max}$ is maximum value of strain at point of unloading, and ε_0 is the static strain. Recovery strain, creep ratio and logarithmic creep/recovery rate were calculated using Eqs. (3)–(5).

$$\varepsilon_{recov} = \varepsilon_{un} - \varepsilon_{res} \tag{3}$$

where ε_{recov} is recovery strain, ε_{un} is static unloading strain and ε_{res} is residual strain

$$Creep\ ratio = \frac{\varepsilon_{\max}}{\varepsilon_0} \tag{4}$$

$$log\ creep \Big/ recovery\ creep\ rate = Creep\ ratio = \frac{\Delta log_{10}\varepsilon(t)_{creep/reccov}}{\Delta t} \tag{5}$$

Other side the normalized stress was calculated using Eq. (6)

$$Normalized\ stress = \frac{\sigma(t)}{\sigma_0} \tag{6}$$

where $\sigma(t)$ is the stress at is any arbitrary time t and σ_0 is a peak stress. Please note that the results represent the mean value of creep strain (n = 12 in both control and T2D).

2.7. Statistical analysis

To compare the results among the groups and to check the significant difference in the obtained parameters among the groups, statistical analysis was performed using the SPSS software (v.21, SPSS Inc. Chicago, IL, USA). The normal distribution of data was checked by the Kolmogorov-Smirnov test, and Student *t*-test was performed to check the statistically significant difference in parameters among the groups. The Pearson correlation test was performed to check the significant relation between the change in mechanical parameters and alteration in molecular structure. This test was performed for T2D and control group separately. The 95 % confidence level was chosen to imply a statistical significance between the groups where $p < 0.05$, $p < 0.01$, and $p < 0.001$ denote the level of significance. Furthermore, in order to identify that among all structural parameters which one was more strongly associated with the macroscopic mechanical properties of tissue, a backward stepwise multiple regression analysis was performed. Initially, the collinearity among the independent variables was checked and then regression models were fitted to a given response parameter (Sihota et al., 2020; Sihota et al., 2021).

3. Results

3.1. Mechanical test

The significant increase in average blood glucose level (HbA1c) ($p = 0.0004$) and decrease in plasma insulin ($p = 0.006$) in one group of rats confirmed the introduction of diabetes in rats. Average weight of control (272 ± 16 g) and T2D (269 ± 21 g) rats was found almost same at the time of sacrifice which indicates the non-obesity of T2D rat.

The strain-time graph in Fig. 2(B) shows the value of strain after loading, creep, unloading, and recovery. The variation of creep with time corresponding to 0.2 % (2000 με) and 0.4 % (4000 με) loading strain in control and diabetic vertebra are demonstrated in Fig. 4(A) and (B), respectively. These figures indicate the significant reduction ($p < 0.05$, $p < 0.01$) of creep strain in T2D rats corresponding to all time points. The value of creep strain at end of creep step and corresponding to 0.2 % loading strain for control and T2D rat were 294.30 ± 53.86 με (n = 6) and 235.19 ± 35.27 με (n = 6), respectively. However, value of creep strain at the end of creep step and corresponding to 0.4 % loading strain for control and T2D rat were 582.10 ± 47. 73 με (n = 6) and 441.52 ± 35.27 με (n = 6), respectively. These value of creep strain corresponding to both loading strain were found significantly different between the control and T2D rat (Table 1). For more accurate comparison of creep response between control and T2D corresponding 0.2 % and 0.4 % loading strain, creep ratio was calculated and its average value is presented in Fig. 4(C). The creep behavior of control and T2D specimens were found independent to loading strain as its value in both control and T2D specimens were not significant different between the 0.2 % and 0.4 % loading strain ($p = 0.82$ for control group and $p = 0.54$ for T2D group). On the other hand, the value of creep ratio was found significantly less in T2D rats than control rats ($p < 0.05$ corresponding to 0.2 % loading strain and $p < 0.01$ corresponding to 0.4 % loading

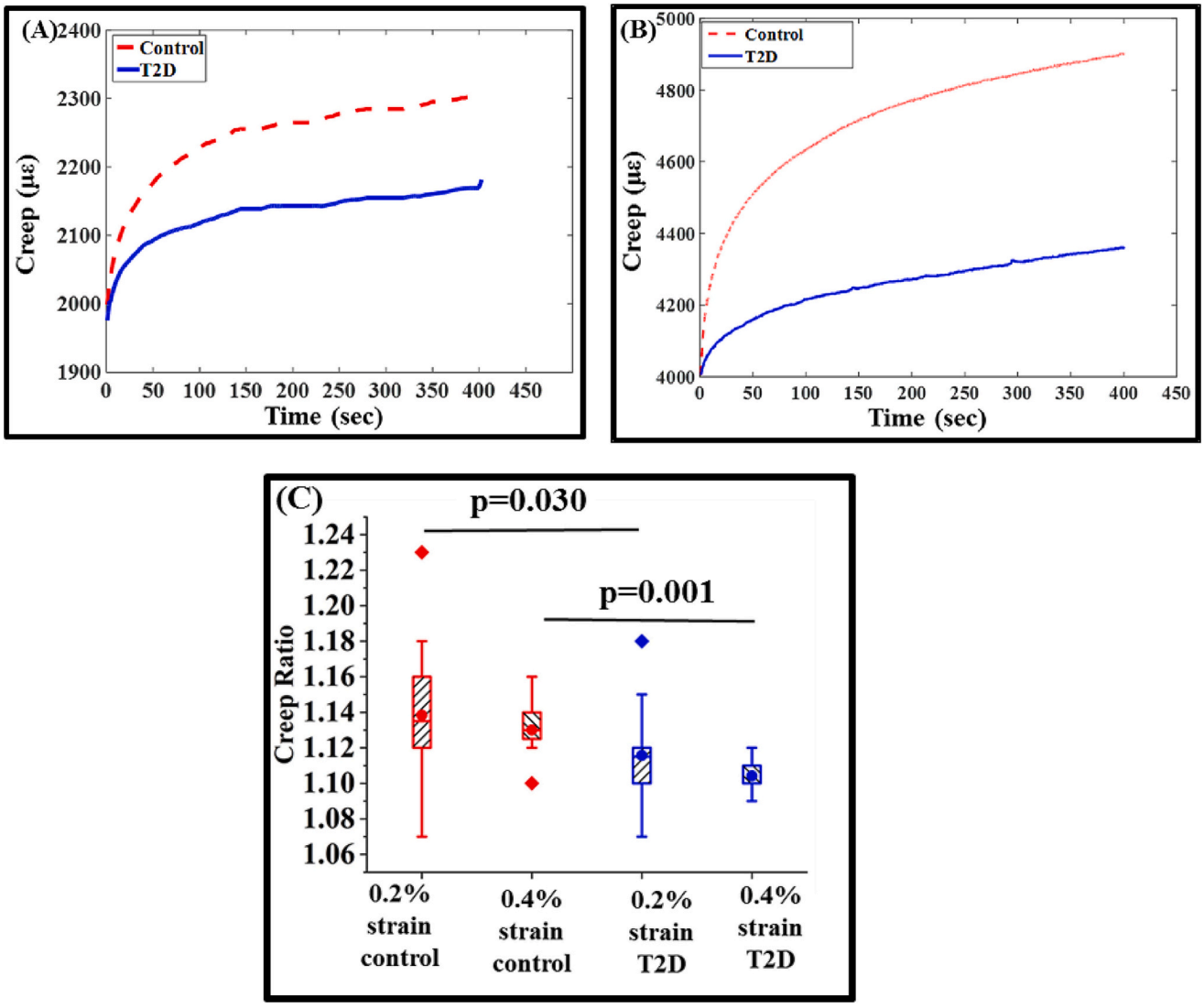

Fig. 4. Creep-time curve for control and T2D specimens corresponding to (A) 2000 and (B) 4000 με initial applied strain. *Note*, these curve present the mean value of creep strain. (C) Comparison of creep ratio (ε(t)/ε(0)) between control and T2D specimens corresponding to 0.2 % (2000 με) and 0.4 % (4000 με). *Note*- p value <0.05 shows statistical significant difference.

strain). Further, creep rate (calculated as a slope of creep curve in the logarithmic scale) was found significantly larger in control specimens than T2D rats ($p < 0.01$). This trend was observed true for both 0.2 % and 0.4 % loading strain (Table 1).

Furthermore, the control specimens showed faster and larger recovery in strain than T2D specimens as the value of recovery rate and recovery strain during zero load hold phase were found larger in control specimens than the T2D specimens (Table 1). This observation was found true for both the loading strain 0.2 % and 0.4 %. The normalized value of recovery strains (recovery strain/applied strain) between 0.2 % and 0.4 % were not found significantly different. The value of normalized recovery strain in control and T2D groups corresponding to 0.2 % loading strain were 0.11 ± 0.02 and 0.11 ± 0.02, respectively; and corresponding to 0.4 % loading strain were 0.12 ± 0.02 and 0.10 ± 0.01, respectively. Further, the value of recovery rate in both control and T2D groups were found significantly larger for 0.4 % loading strain than 0.2 % loading strain (Table 1). Also, the value of residual strain after 600 s of recovery period was larger in control specimens than the T2D specimens. However, its normalized values in both control and T2D specimens were not found significantly different between 0.2 % and 0.4 % loading strains.

The results of stress relaxation experiment for control and T2D specimens are shown in Fig. 5. Fig. 5(A) presents the mean value of normalized stress during hold phase in control and T2D specimens. In control specimens the stress was found continuously decreasing with time, whereas in T2D specimens the stress relaxation curve became plateau after initial hold phase (say 600 s). The mean value of stress relaxation after 600 s for control and T2D rats were 46.6 % and 43.2 %, respectively and these values were found significantly different between T2D rats and control rats (Fig. 5(B)).

3.2. Molecular structure

The representative ATR-FTIR spectrum of bone is shown in Fig. 3(A) whereas the de-convoluted amide-I (1590–1710 cm^{-1}) band of the representative ATR-FTIR spectrum is shown in Fig. 3(B). Table 2 presents the compression of molecular structural parameters between control and T2D specimens. Mineral-to-matrix ratio (mineralization) ($p = 0.02$) and carbonate-to-phosphate ratio (carbonate substitution) ($p < 0.01$) were found significantly larger in T2D group than the control group. The mean value of mineral-to-matrix ratio for control and T2D was 2.93 and 3.72, respectively whereas mean value of carbonate-to-

Table 1
Creep parameters corresponding to 0.2 % and 0.4 % for control and T2D groups.

	0.2 % (2000 με) strain			0.4 % (4000 με) strain		
Parameters/ groups	Control	T2D	p-value	Control	T2D	p-value
Peak stress (MPa)	0.51 ± 0.08	0.86 ± 0.15	<0.01	1.54 ± 0.27	2.17 ± 0.31	<0.01
Loading modulus (MPa)	282.05 ± 54.86	468.34 ± 78.79	<0.01	406.54 ± 22.86	606.52 ± 25.22	<0.01
Unloading modulus (MPa)	438.42 ± 91.34	644.01 ± 115.21	<0.01	579.10 ± 87.80	755.52 ± 88.14	<0.01
Creep strain (με)	294.30 ± 53.86	235.19 ± 38.57	<0.01	582.10 ± 47.73	441.52 ± 35.27	<0.01
Recovery strain (με)	224.16 ± 35.41	211.12 ± 35.15	<0.01	465.14 ± 80.57	388.53 ± 26.07	<0.01
Residual strain (με)	575.06 ± 75.79	648.51 ± 61.72	<0.05	729.23 ± 55.27	836.83 ± 43.50	<0.01
Log creep rate	0.028 ± 0.008	0.023 ± 0.002	<0.01	0.03 ± 0.01	0.021 ± 0.002	<0.01
Log recovery rate	0.053 ± 0.003	0.035 ± 0.003	<0.01	0.080 ± 0.01	0.07 ± 0.001	<0.01

Note – difference in the parameters was considered significant for p value <0.05.

phosphate ratio (carbonate substitution) was 0.014 and 0.017, respectively. However, disease-related changes in mineral crystallinity, acid phosphate content, and collagen maturity were not found significant. Further, the amount of non-enzymatic cross links was found significantly increased ($p = 0.01$) in T2D group whereas the amount of enzymatic cross links in T2D groups was observed significantly decreased ($p < 0.01$). Furthermore, the comparison of mineral crystal length and width (obtained through XRD) between control and T2D specimens is shown in Fig. 6(A&B). No significant alterations due to T2D were found in the crystal length ($p = 0.22$) and width ($p = 0.39$).

3.3. Relationship between molecular structure composition and mechanical properties

Increase in elastic modulus in T2D group was found in correlation with increase in mineralization ($r = 0.78$, $p < 0.01$) (Fig. 7(A)). Moreover, the logarithmic creep rate was found negatively correlated with the amount of NE-xL ($r = -0.94$, $p < 0.01$) and residual strain ($r = -0.93$, $p < 0.01$) (Fig. 7(B&C)). Correlation between the amount of enzymatic cross link and mechanical properties was not found significant ($r = 0.21$, $p > 0.05$). Other molecular structural parameters were also not found significantly correlated with the mechanical properties. The amount of stress relaxation was found inversely correlated with the non-enzymatic cross links and mineralization ($r = -0.98$, $p < 0.01$ for control rats and $r = -0.95$, $p < 0.05$ for T2D rats) (see Fig. 8). Further, multiple regression analysis showed that out of the above measured structural parameters, mineral to matrix ratio was found strongly and positively correlated to elastic modulus ($r = 0.93$, $p < 0.01$), whereas NE-xL was found strongly negatively correlated with the viscoelastic properties (e.g. creep rate ($r = -0.97$, $p < 0.01$), residual strain ($r = -0.98$, $p < 0.01$) and stress relaxation ($r = -0.95$, $p < 0.01$)).

4. Discussion

In current study, we have investigated the effect of T2D on the compositional and viscoelastic property of vertebral bone. In this study static creep and stress relaxation experiments were performed to understand effect of T2D on the viscoelastic behavior of vertebra. The obtained results demonstrate that T2D alters viscoelastic behavior of vertebra as amount of creep, recovery and stress relaxation are significantly lower in case of T2D. This study also shows that the viscoelastic behavior of vertebra is linear as it is found insensitive to the applied strain. Here, the cause of alteration in viscoelastic properties of vertebra is explained in terms of its compositional properties.

Rat vertebrae segments are small in length and embedding its end with plate may affect the boundary conditions during the compression experiments due to small value of gauge length. On the other hand, obtaining true plano-parallel surfaces is difficult for such small specimens (Brouwers et al., 2009), to ensure proper contact between specimens and grip surface. Plano-parallel surface of the specimens are important to allow the uniform distribution of applied compressive force over the specimen cross section. Therefore, to preparing the plano-

Table 2
Compression of molecular structure parameters between Control and T2D group.

Molecule structure parameter	Control	T2D	p-value
Mineral:matrix	2.93 ± 0.78	3.72 ± 0.53	<0.05
Carbonate to phosphate (852-890/916-1180)	0.014 ± 0.003	0.017 ± 0.002	<0.01
Mineral crystalinity (1030/1020)	0.88 ± 0.03	0.91 ± 0.02	>0.05
Acid phosphate content (1127/1096)	0.32 ± 0.05	0.29 ± 0.05	>0.05
Collagen maturity	2.96 ± 0.08	2.96 ± 0.41	>0.05
Enzymatic cross linking (E-xLR)	3.73 ± 1.53	1.68 ± 0.31	<0.01
Nonenzymatic cross link ratio (NE-xLR)	1.53 ± 0.07	3.84 ± 0.20	<0.01

Note – difference in the parameters was considered significant for p value <0.05.

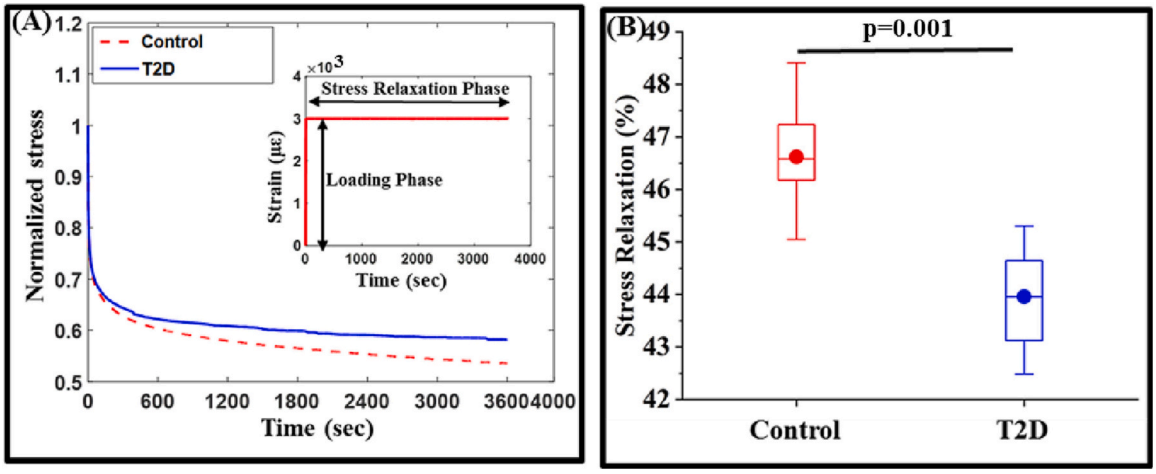

Fig. 5. (A) Presents the trend of stress relaxation in control and T2D specimens. This graph presents mean value of normalized stress. (B) Comparison of amount of stress relaxation between control and T2D specimens.

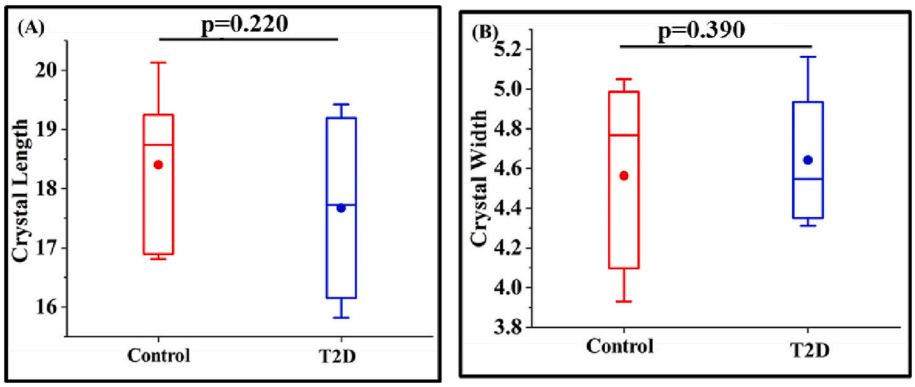

Fig. 6. Comparison of (A) mean crystal length and (B) mean crystal width between control and T2D vertebral specimens.

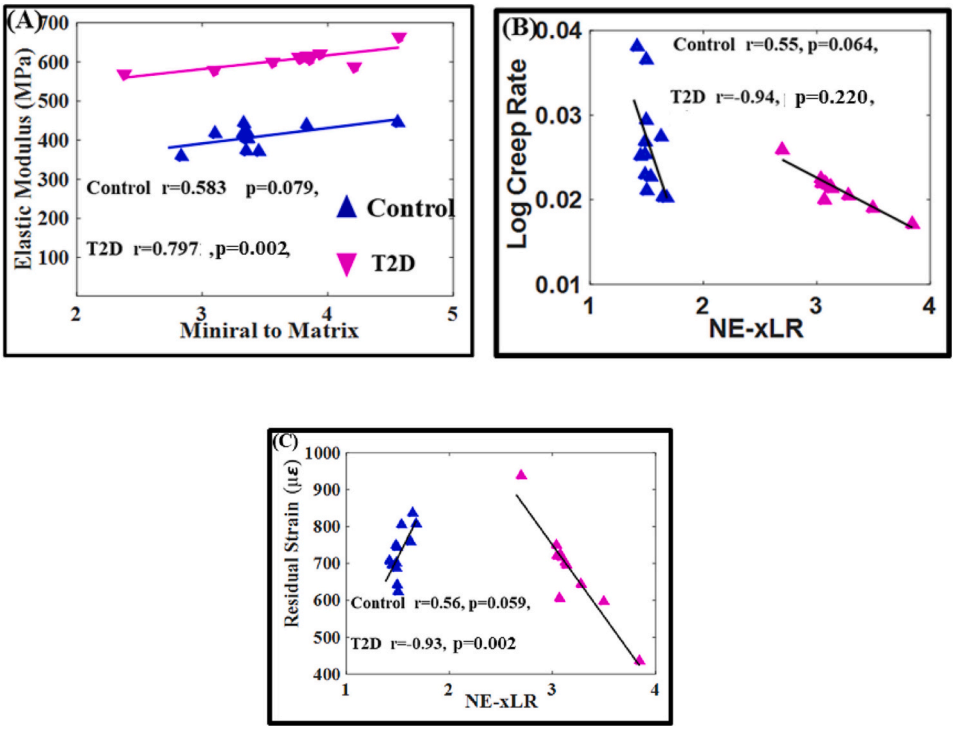

Fig. 7. Correlation between (A) elastic modulus and matrix to mineral ratio, (B) log creep rate and non-enzymatic cross link (NE-xLR) and (C) residual strain and non-enzymatic cross link (NE-xLR).

parallel surfaces with constant gauge length among all specimens, we used similar method as described in literature. During the cutting, vibration and heat generation may affect the surface microstructure, therefore we used ultra-slow cutting speed with continuous irrigation of PBS to minimize the cutting effect on the tissue microstructure (Yadav et al., 2021; Karim et al., 2013; Sihota et al., 2019).

Before moving to the viscoelastic properties, initially the apparent Young's modulus is compared between control and T2D specimens of the vertebrae to confirm the validity of the performed experiments. The value of apparent Young's modulus is significantly large in T2D specimens, which is found in good agreement with the available literature (Sihota et al., 2020; Yadav et al., 2021). These values are also found in the range of reported values of vertebra modulus (Kurutzné Kovács et al., 2004; Yeni and Fyhrie, 2001). However other studies reported the decreased stiffness in T2D vertebra (Acevedo et al., 2018; Karim et al., 2013; Fields et al., 2015; Broz et al., 2021). This inconsistency between our result and literature can be the results of different in animal model used. In literature, the increase in modulus in T2D case is related to increase in mineral to matrix ratio (Sihota et al., 2020). In the current study, we also compare the compositional properties between control and T2D groups, where a significant increase in mineral to matrix ratio and NE-xLR is observed in T2D specimens.

Other structural parameters such as crystal length and width may also contribute to elastic properties of bone tissue (Sihota et al., 2020; Yamamoto et al., 2009; Yadav et al., 2021), which are also measured for both the groups. These two crystal structural parameters are not found significantly different between control and T2D specimens, therefore it can be speculated that the increase in modulus is the result of increase in mineral to matrix ratio. Pearson correlation test confirms this hypothesis as a positive linear correlation was found between mineral to matrix ratio and elastic modulus. The non-enzymatic crosslinking is associated with the decrease in mechanical properties of bone (Karim and Bouxsein, 2016; Nyman et al., 2007).The previous studies has reported the increase in bone brittleness and reduction in post yield displacement due increase in non-enzymatic cross links (Vashishth et al., 2001). The similar observation were observed on ex-vivo glycation studies that post

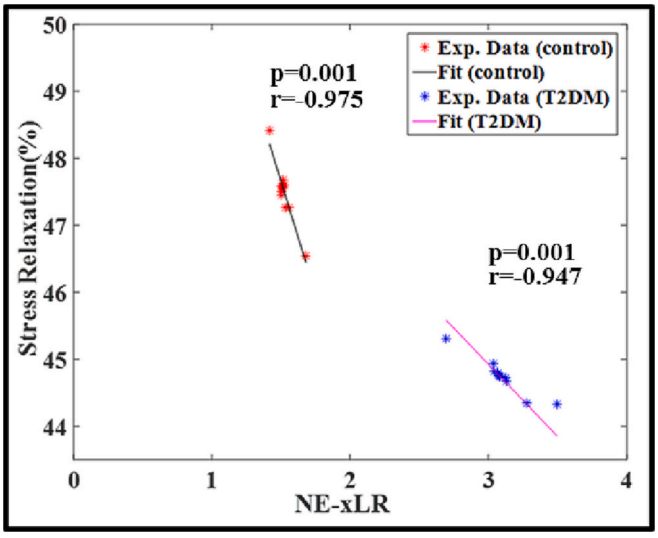

Fig. 8. Correlation between stress relaxation and non-enzymatic cross link (NE-xLR).

yield strength and post-yield energy of bone reduces with increase in non-enzymatic crosslinking (Tang et al., 2007; Tang and Vashishth, 2010).

Furthermore, the non-enzymatic cross linking restricts molecular/collagen fibril sliding and subsequently influences the post-yield behavior of bone (Acevedo et al., 2018; Reinwald et al., 2009; Karim and Vashishth, 2012; Sroga et al., 2015; Tang and Vashishth, 2011; Palomino et al., 2018; Hammond et al., 2014). Here, the non-enzymatic crosslinking is found to influence the viscoelastic behavior of bone. With the increase in non-enzymatic cross-linking, reduction in creep strain and recovery strain is observed. A previous study has also observed the reduced stress relaxation as a results of non-enzymatic glycations (Jia et al., 2021). The viscoelasticity of bone is primarily associated with its organic phase, water phase and hierarchical microstructure. The sliding and slippage between collagen and mineral phases at different length scales also contributes to viscoelastic deformation of bone. However with the accumulation of non-enzymatic crosslinking, these deformations are restricted which subsequently reduces the viscoelastic deformation of bone.

The viscoelastic materials dissipate energy when subjected to load. In bone, this is important for providing resistance against the fracture under the dynamic or impact loading condition. In this study, we investigated the alteration in creep and stress relaxation behavior of vertebra due to T2D. The creep behavior is associated with the long-term deformation of vertebra, whereas stress relaxation is associated with stress dissipation during the long time straining of vertebra due to its physiological loading. The previous study by Kim et al. (2011) found that a large amount of creep induced in the vertebra under the physiological applied load and about half of strain does not recover after complete unloading, which remains as a residual strain. These findings suggested that the progressive vertebral deformation (residual strain) would be developed even at the physiological loading level over the years, which may increase the risk of vertebral fracture.

The results of this study show that creep related parameters such as creep strain, creep rate, recovery strain, recovery rate and residual strain were found altered in T2D samples. For the same value of applied strains (2000 με or 4000 με), the value of creep strain, creep rate, recovery strain, and recovery rate were found significantly less in T2D group. Moreover, the residual strain after complete unloading is significantly more in T2D specimens. Further, the one hour stress relaxation experiment shows that the amount of stress dissipation is significantly less in T2D specimens. A study published by Kim et al. (2011) demonstrated that microstructure of vertebra affects its viscoelastic behavior. Further, our group (Sihota et al., 2020; Sihota et al., 2019; Yadav et al., 2022) disclosed that T2D alters the mechanical properties of bone and this alteration is associated with its micro and molecular structure. We have investigated the vertebra molecular structure. Statistical analysis results show a significant increase in mineral to matrix ratio, carbonate to phosphate ratio, and NE-xLR with T2D, whereas the amount of E-xLR is found less in T2D specimens. These microstructural observations are found in good agreement with the viscoelastic properties. Further, the mineral crystallinity and crystal size (length and width) are not found significantly different between control and T2D. Moreover, the results of this study show that the viscoelastic parameters are associated with molecular parameters of the vertebra. The logarithmic creep rate was found strongly correlated with the mineral to matrix ratio and NE-xLR as its value is found linearly decreasing with increase in mineral to matrix and NE-xLR. These results indicate that increase in mineral to matrix ratio and NE-xLR restrict the relative or gradual sliding/deformation among the constituents. Further, it can also be believed that the NE-xLR affect the molecular mobility and capability of change in conformations and rearrangements of the molecules against the applied load which leads to reduction in creep capability of vertebra (Reinwald et al., 2009; Kurutzné Kovács et al., 2004; Hammond et al., 2014; Gonzalez et al., 2014). This alteration in bone molecular results in an increase in brittleness which makes vertebra bone prone to fracture. This behavior of vertebra can also be confirmed with the stiffening behavior of bone in T2D groups where specimens corresponding to high linear modulus show less creep and less stress recovery than the specimens with low linear modulus. Further, the residual strain is found statistically correlated with the NE-xLR as its value is found linearly increasing with increase in NE-xLR. This result indicates that increase in cross link will reduce the shape memory behavior of bone which could be due to the irreversible damage in the microstructure of tissue. The recovery rate is also found slow in T2D samples which could be due to the increase in non-enzymatic cross link density. These unwanted cross links increase the brittleness of the tissue.

Further, the stress relaxation behavior of the vertebra is also found altered in T2D specimens, where the amount of stress relaxation is found strongly correlated with the NE-xLR. The stress relaxation of vertebra is found linearly decreasing with increase in NE-xLR. The stress relaxation against the constant hold strain occurs due to the redistribution of applied strain within the constituents of tissue. This strain redistribution phenomenon generally may occur due to the sliding of constituents over each other (Yadav et al., 2022; Dwivedi et al., 1881). Therefore, it can be speculated that the NE-xLR constrained the sliding of constituents and then deteriorates the dissipation capacity of tissue. The alteration in bone structure makes it prone to fracture.

This study also investigated the effect of loading strain on the creep behavior of vertebra The obtained results show that the creep ratio is found independent to the applied strain, whereas the residual strain is found increasing with increase in applied strain. These results show that the irreversible damage of tissue increases with increase in the value of applied strain. Further, the increase in residual strain with applied strain is more in T2D specimens which indicate more irreversible damage. Overall this study demonstrated that the T2D affects the viscoelastic properties of vertebra which may lead to alteration in its physiological functions such as protection against the dynamic load and impact load.

Despite our study presents some new data related to effect of T2D on vertebra viscoelastic behavior, this study has numerous limitations. First, the use of low-dose STZ causes a partial loss of pancreatic beta cell by direct cytotoxic action (unlikely T2D in humans) [reference]. Also, low-dose STZ is only effective to induce diabetes in HFD-fed insulin-resistant rats and fails to induce diabetes in normal control rats. The use of high STZ dose may cause absolute deficiency in insulin which is a characteristic of type 1 diabetes in lieu of type 2 diabetes, thus we used low dose of STZ in our study. Other reason to use low dose STZ is to develop late stage of T2D condition in limited period of time. Second, we measured the viscoelastic properties under static loading however

vertebra is also subjected to dynamic loading therefore, understanding the T2D associated alteration in viscoelastic behavior of vertebra under dynamic loading is also important. In this study we did not investigated the microstructure of control and T2D vertebra though knowledge of correlation between vertebra viscoelastic behavior and its microstructure will provide more insight in to T2D associated alteration in vertebral biomechanics. Therefore, in future the detail studies are required to understand the effect of T2D on the vertebra viscoelastic behavior and its structural response. Last but not least, the origin of brittle fracture vertebra caused by T2D is important to care the vertebra bone which is not investigated in this study. Therefore, in future, a separate detail work is need to address cause of brittle fracture in T2D vertebra.

5. Conclusion

This study investigated the effects of T2D on the viscoelastic behavior of vertebra some of the drawn conclusions from this study are listed below

- T2D makes the vertebra more brittle which is due to the increase in mineral-to-matrix ratio and NE-xLR.
- The creep behavior of tissue is also found to deteriorate in T2D specimens where the amount of creep and its rate is significantly less.
- The T2D specimens show more irreversible damage during the static loading and the value of recovery and residual strains are small and large in T2D specimens, respectively.
- The T2D restricts the internal sliding and mobility of the constituents (collagen fiber) which decreases the stress dissipation capacity of vertebra and hence makes it more prone to fracture.
- The viscoelastic response of vertebra is found independent to the applied strain as a significant difference is not found in the value of creep ratio between control and T2D specimens.

CRediT authorship contribution statement

Deepak Mehta:
Writing – review & editing, Writing – original draft, Visualization, Validation, Software, Methodology, Investigation, Formal analysis, Data curation, Conceptualization
Praveer Sihota
Visualization, review
Kulbhushan Tikoo,
Sources
Sachin Kumar
Supervision and editing
Navin Kumar
Sources

Declaration of competing interest

The authors declare that they have no known competing financial interests or personal relationships that could have appeared to influence the work reported in this paper.

Data availability

Data will be made available on request.

Acknowledgements

The authors acknowledge highly to IIT Ropar for providing the necessary facilities used in this study. The authors would like to acknowledge Mr. Piyush Uniyal and Aakash Soni for their help in rectifying the language. The authors also would like to acknowledge Mr. Sushil Kumar for their help in FTIR-ATR, Mr. Amit Kamboj for his help in experiments.

References

Acevedo, C., Sylvia, M., Schaible, E., Graham, J.L., Stanhope, K.L., Metz, L.N., et al., 2018. Contributions of material properties and structure to increased bone fragility for a given bone mass in the UCD-T2DM rat model of type 2 diabetes. J. Bone Miner. Res. 33 (6), 1066–1075.
Anekstein, Y., Smorgick, Y., Lotan, R., Agar, G., Shalmon, E., Floman, Y., et al., 2010. Diabetes mellitus as a risk factor for the development of lumbar spinal stenosis. Israel Med. Assoc. J. 12 (1), 16.
Briggs, A.M., Greig, A.M., Wark, J.D., Fazzalari, N.L., Bennell, K.L., 2004. A review of anatomical and mechanical factors affecting vertebral body integrity. Int. J. Med. Sci. 1 (3), 170.
Brouwers, J.E.M., Ruchelsman, M., Rietbergen, B.V., Bouxsein, M.L., 2009. Determination of rat vertebral bone compressive fatigue properties in untreated intact rats and zoledronic-acid-treated, ovariectomized rats. Osteoporos Int. 20, 1377–1384.
Browne, J.A., Cook, C., Pietrobon, R., Bethel, M.A., Richardson, W.J., 2007. Diabetes and early postoperative outcomes following lumbar fusion. Spine (Phila Pa 1976) 32 (20), 2214–2219.
Brownlee, M.D.M., 1995. Advanced protein glycosylation in diabetes and aging. Annu. Rev. Med. 46 (1), 223–234.
Broz, K., Walk, R.E., Tang, S.Y., 2021. Complications in the spine associated with type 2 diabetes: the role of advanced glycation end-products. Med. Nov. Technol. Dev. 11, 100065.
Care, D., Suppl, S.S., 2019. In: Introduction : Standards of Medical Care in Diabetes d 2019, 42, pp. 2018–2019 (December 2018).
Dwivedi, K.K., Lakhani, P., Kumar, S., Kumar, N., 1881. In: The Effect of Strain Rate on the Stress Relaxation of the Pig Dermis: A Hyper-viscoelastic Approach, pp. 1–44.
Fields, A.J., Berg-Johansen, B., Metz, L.N., Miller, S., La, B., Liebenberg, E.C., et al., 2015. Alterations in intervertebral disc composition, matrix homeostasis and biomechanical behavior in the UCD-T2DM rat model of type 2 diabetes. J. Orthop. Res. 33 (5), 738–746.
Gallant, M.A., Brown, D.M., Organ, J.M., Allen, M.R., Burr, D.B., 2013. Reference-point indentation correlates with bone toughness assessed using whole-bone traditional mechanical testing. Bone 53 (1), 301–305.
Gonzalez, A.D., Gallant, M.A., Burr, D.B., Wallace, J.M., 2014. Multiscale analysis of morphology and mechanics in tail tendon from the ZDSD rat model of type 2 diabetes. J. Biomech. 47 (3), 681–686.
Gustafson, H.M., Melnyk, A.D., Siegmund, G.P., Cripton, P.A., 2017. Damage identification on vertebral bodies during compressive loading using digital image correlation. Spine (Phila Pa 1976) 42 (22), E1289–E1296.
Hammond, M.A., Gallant, M.A., Burr, D.B., Wallace, J.M., 2014. Nanoscale changes in collagen are reflected in physical and mechanical properties of bone at the microscale in diabetic rats. Bone 60, 26–32.
Hunt, H.B., Pearl, J.C., Diaz, D.R., King, K.B., Donnelly, E., 2018. Bone tissue collagen maturity and mineral content increase with sustained hyperglycemia in the KK-ay murine model of type 2 diabetes. J. Bone Miner. Res. 33 (5), 921–929.
Hunt, H.B., Torres, A.M., Palomino, P.M., Marty, E., Saiyed, R., Cohn, M., et al., 2019. Altered tissue composition, microarchitecture, and mechanical performance in cancellous bone from men with type 2 diabetes mellitus. J. Bone Miner. Res. 34 (7), 1191–1206.
Jia, S., Gong, H., Cen, H., Shi, P., Zhang, R., Li, Z., et al., 2021. Influence of non-enzymatic glycation on the mechanical properties of cortical bone. J. Mech. Behav. Biomed. Mater. 119, 104553.
Kanazawa, I., Yamaguchi, T., Yamamoto, M., Yamauchi, M., Yano, S., Sugimoto, T., 2009. Relationships between serum adiponectin levels versus bone mineral density, bone metabolic markers, and vertebral fractures in type 2 diabetes mellitus. Eur. J. Endocrinol. 160 (2), 265.
Karim, L., Bouxsein, M.L., 2016. Effect of type 2 diabetes-related non-enzymatic glycation on bone biomechanical properties. Bone 82, 21–27.
Karim, L., Vashishth, D., 2012. Heterogeneous glycation of cancellous bone and its association with bone quality and fragility. PLoS One 7 (4), e35047.
Karim, L., Tang, S.Y., Sroga, G.E., Vashishth, D., 2013. Differences in non-enzymatic glycation and collagen cross-links between human cortical and cancellous bone. Osteoporos. Int. 24, 2441–2447.
Karim, L., Moulton, J., Van Vliet, M., Velie, K., Robbins, A., Malekipour, F., et al., 2018. Bone microarchitecture, biomechanical properties, and advanced glycation end-products in the proximal femur of adults with type 2 diabetes. Bone 114, 32–39.
Keaveny, T.M., Wachtel, E.F., Ford, C.M., Hayes, W.C., 1994. Differences between the tensile and compressive strengths of bovine tibial trabecular bone depend on modulus. J. Biomech. 27 (9), 1137–1146.
Keller, T.S., Harrison, D.E., Colloca, C.J., Harrison, D.D., Janik, T.J., 2003. Prediction of osteoporotic spinal deformity. Spine (Phila Pa 1976) 28 (5), 455–462.
Kim, D.-G., Shertok, D., Tee, B.C., Yeni, Y.N., 2011. Variability of tissue mineral density can determine physiological creep of human vertebral cancellous bone. J. Biomech. 44 (9), 1660–1665.
Klotzbuecher, C.M., Ross, P.D., Landsman, P.B., Abbott III, T.A., Berger, M., 2000. Patients with prior fractures have an increased risk of future fractures: a summary of the literature and statistical synthesis. J. Bone Miner. Res. 15 (4), 721–739.
Kurra, S., Siris, E., 2011. Diabetes and bone health: the relationship between diabetes and osteoporosis-associated fractures. Diabetes Metab. Res. Rev. 27 (5), 430–435.
Kurutzné Kovács, M., Fornet, B., Gálos, M., 2004. Compressive Load Bearing and Bone Architecture of Lumbar Vertebrae in Terms of Sex and Aging.
Lakhani, P., Sihota, P., Tikoo, K., Kumar, S., Kumar, N., et al., 2023. The multiscale characterization and constitutive modeling of healthy and type 2 diabetes mellitus Sprague Dawley rat skin. Acta Biomater. 158, 324–346.

Li, J., Huang, S., Tang, Y., Wang, X., Pan, T., 2017. Biomechanical analysis of the posterior bony column of the lumbar spine. J. Orthop. Surg. Res. 12 (1), 1–7.
Liu, X., Pan, F., Ba, Z., Wang, S., Wu, D., 2018. The potential effect of type 2 diabetes mellitus on lumbar disc degeneration: a retrospective single-center study. J. Orthop. Surg. Res. 13 (1), 1–5.
Melton III, L.J., Kallmes, D.F., 2006. Epidemiology of vertebral fractures: implications for vertebral augmentation. Acad. Radiol. 13 (5), 538–545.
Miyake, H., Kanazawa, I., Sugimoto, T., 2018. Association of bone mineral density, bone turnover markers, and vertebral fractures with all-cause mortality in type 2 diabetes mellitus. Calcif. Tissue Int. 102 (1), 1–13.
Molsted, S., Tribler, J., Snorgaard, O., 2012. Musculoskeletal pain in patients with type 2 diabetes. Diabetes Res. Clin. Pract. 96 (2), 135–140.
Nyman, J.S., Roy, A., Tyler, J.H., Acuna, R.L., Gayle, H.J., Wang, X., 2007. Age-related factors affecting the postyield energy dissipation of human cortical bone. J. Orthop. Res. 25 (5), 646–655.
O'Callaghan, P., Szarko, M., Wang, Y., Luo, J., 2018. Effects of bone damage on creep behaviours of human vertebral trabeculae. Bone 106, 204–210.
Oravec, D., Kim, W., Flynn, M.J., Yeni, Y.N., 2018. The relationship of whole human vertebral body creep to geometric, microstructural, and material properties. J. Biomech. 73, 92–98.
Palomino, P., Hunt, H., Marty, E., Saiyed, R., Cohn, M., Lane, J., et al., 2018. Advanced glycation endproduct content is increased in cortical bone of the femoral neck in men with type 2 diabetes mellitus. J. Bone Miner. Res. 13.
Piccoli, A., Cannata, F., Strollo, R., Pedone, C., Leanza, G., Russo, F., et al., 2020. Sclerostin regulation, microarchitecture, and advanced glycation end-products in the bone of elderly women with type 2 diabetes. J. Bone Miner. Res. 35 (12), 2415–2422.
Pollintine, P., Luo, J., Offa-Jones, B., Dolan, P., Adams, M.A., 2009. Bone creep can cause progressive vertebral deformity. Bone 45 (3), 466–472.
Reinwald, S., Peterson, R.G., Allen, M.R., Burr, D.B., 2009. Skeletal changes associated with the onset of type 2 diabetes in the ZDF and ZDSD rodent models. Am. J. Physiol. Metab. 296 (4), E765–E774.
Robinson, D.L., Tse, K.M., Franklyn, M., Zhang, J., Fernandez, J.W., Ackland, D.C., et al., 2021. Specimen-specific fracture risk curves of lumbar vertebrae under dynamic axial compression. J. Mech. Behav. Biomed. Mater. 118, 104457.
Rubin, M.R., Paschalis, E.P., Poundarik, A., Sroga, G.E., McMahon, D.J., Gamsjaeger, S., et al., 2016. Advanced glycation endproducts and bone material properties in type 1 diabetic mice. PLoS One 11 (5), e0154700.
Schmidt, F.N., Zimmermann, E.A., Campbell, G.M., Sroga, G.E., Püschel, K., Amling, M., et al., 2017. Assessment of collagen quality associated with non-enzymatic cross-links in human bone using fourier-transform infrared imaging. Bone 97, 243–251.
Sihota, P., Yadav, R.N., Dhiman, V., Bhadada, S.K., Mehandia, V., Kumar, N., 2019. Investigation of diabetic patient's fingernail quality to monitor type 2 diabetes induced tissue damage. Sci. Rep. 9 (1), 3193.
Sihota, P., Yadav, R.N., Poleboina, S., Mehandia, V., Bhadada, S.K., Tikoo, K., et al., 2020. Development of HFD-Fed/Low-dose STZ-treated female Sprague-Dawley rat model to investigate diabetic bone fragility at different organization levels. JBMR Plus. 4 (10), e10379.
Sihota, P., Yadav, R.N., Dhaliwal, R., Bose, J.C., Dhiman, V., Neradi, D., et al., 2021. Investigation of mechanical, ma1. Sihota P et al. 2021 Investigation of mechanical, material and compositional determinants of human trabecular bone quality in type 2 diabetes. J. Clin. Endocrinol. Metab.
Sone, T., Tomomitsu, T., Miyake, M., Takeda, N., Fukunaga, M., 1997. Age-related changes in vertebral height ratios and vertebral fracture. Osteoporos. Int. 7 (2), 113–118.
Sroga, G.E., Siddula, A., Vashishth, D., 2015. Glycation of human cortical and cancellous bone captures differences in the formation of Maillard reaction products between glucose and ribose. PLoS One. 10 (2), e0117240.
Tang, S.Y., Vashishth, D., 2010. Non-enzymatic glycation alters microdamage formation in human cancellous bone. Bone 46 (1), 148–154.
Tang, S.Y., Vashishth, D., 2011. The relative contributions of non-enzymatic glycation and cortical porosity on the fracture toughness of aging bone. J. Biomech. 44 (2), 330–336.
Tang, S.Y., Zeenath, U., Vashishth, D., 2007. Effects of non-enzymatic glycation on cancellous bone fragility. Bone 40 (4), 1144–1151.
Tsai, T.-T., Ho, N.Y.-J., Lin, Y.-T., Lai, P.-L., Fu, T.-S., Niu, C.-C., et al., 2014. Advanced glycation end products in degenerative nucleus pulposus with diabetes. J. Orthop. Res. 32 (2), 238–244.
Vashishth, D., Gibson, G.J., Khoury, J.I., Schaffler, M.B., Kimura, J., Fyhrie, D.P., 2001. Influence of nonenzymatic glycation on biomechanical properties of cortical bone. Bone 28 (2), 195–201.
Wölfel, E.M., Jähn-Rickert, K., Schmidt, F.N., Wulff, B., Mushumba, H., Sroga, G.E., et al., 2020. Individuals with type 2 diabetes mellitus show dimorphic and heterogeneous patterns of loss in femoral bone quality. Bone 140, 115556.
Wyatt, L.H., Ferrance, R.J., 2006. The musculoskeletal effects of diabetes mellitus. J. Can. Chiropr. Assoc. 50 (1), 43.
Xue, Y., Baker, A.L., Nader, S., Orlander, P., Sanchez, A.J., Kellam, J., et al., 2018. Lumbar spine trabecular bone score (TBS) reflects diminished bone quality in patients with diabetes mellitus and oral glucocorticoid therapy. J. Clin. Densitom. 21 (2), 185–192.
Yadav, R.N., Sihota, P., Uniyal, P., Neradi, D., Bose, J.C., Dhiman, V., et al., 2021. Prediction of mechanical properties of trabecular bone in patients with type 2 diabetes using damage based finite element method. J. Biomech. 123, 110495.
Yadav, R.N., Sihota, P., Neradi, D., Bose, J.C., Dhiman, V., Karn, S., et al., 2022. Effects of type 2 diabetes on the viscoelastic behavior of human trabecular bone. Med. Eng. Phys. 104, 103810.
Yamamoto, E., Crawford, R.P., Chan, D.D., Keaveny, T.M., 2006. Development of residual strains in human vertebral trabecular bone after prolonged static and cyclic loading at low load levels. J. Biomech. 39 (10), 1812–1818.
Yamamoto, M., Yamaguchi, T., Yamauchi, M., Sugimoto, T., 2009. Low serum level of the endogenous secretory receptor for advanced glycation end products (esRAGE) is a risk factor for prevalent vertebral fractures independent of bone mineral density in patients with type 2 diabetes. Diabetes Care 32 (12), 2263–2268.
Yeni, Y.N., Fyhrie, D.P., 2001. Finite element calculated uniaxial apparent stiffness is a consistent predictor of uniaxial apparent strength in human vertebral cancellous bone tested with different boundary conditions. J. Biomech. 34 (12), 1649–1654.